RESEARCH ARTICLE

Antifungal Activity of Iron-gold and Cobalt-gold co-doped ZnO Nanoparticles

A. Ferin Fathima[1,2], R. Jothi Mani[1,3], K. Sakthipandi[4,*]

[1]Department of Physics, Sadakathullah Appa College, Tirunelveli 627 011, Tamil Nadu, India
[2]Manonmanium Sundaranar University, Tirunelveli 627 012, Tamil Nadu, India
[3]Department of Physics, Fatima College, Madurai 625 018, Tamil Nadu, India
[4]Department of Physics, Gandhigram Rural Institute (Deemed to be University), Gandhigram 624 302, Tamil Nadu, India

*Corresponding author: E-mail: sakthipandi@gmail.com; Tel.: (+91) 9944585960

DOI: 10.5185/amlett.2021.061636

$Zn_{0.98}Fe_{0.01}Au_{0.01}O$ and $Zn_{0.98}Co_{0.01}Au_{0.01}O$ nanoparticles (NPs) have been synthesized via poly ethylene glycol assisted route. The average crystallite size of $Zn_{0.98}Fe_{0.01}Au_{0.01}O$ and $Zn_{0.98}Co_{0.01}Au_{0.01}O$ NPs were estimated from X-ray diffraction results and the values are 31.38 nm and 36.14 nm respectively. The UV absorption spectra confirmed the formation of the NPs with the characteristic peaks at 374 and 366 nm respectively. This spectral observation indicates that the band gap of ZnO nanoparticles decreases by doping iron/gold and cobalt/gold nanoparticles. The morphology and elemental composition of $Zn_{0.98}Fe_{0.01}Au_{0.01}O$ and $Zn_{0.98}Co_{0.01}Au_{0.01}O$ NPs were investigated. The antifungal activity of synthesized $Zn_{0.98}Fe_{0.01}Au_{0.01}O$ and $Zn_{0.98}Co_{0.01}Au_{0.01}O$ NPs were found against four postharvest pathogenic fungi like *Aspergillus niger, Aspergillus flavus, Rhizopus microsporus* and *Pencillium sp.* The doping of iron and gold in ZnO nanoparticles enhances the zone of inhibition for the fungal pathogens compared to pure ZnO nanoparticles. Antifungal activity of $Zn_{0.98}Fe_{0.01}Au_{0.01}O$ and $Zn_{0.98}Co_{0.01}Au_{0.01}O$ nanoparticles were higher when compared with standard antibiotic *mycostatin* whose zone of inhibition is 18 mm against *Aspergillus niger, Aspergillus flavus, Rhizopus microsporus* and *Pencillium* sp.

Introduction

In the past decade research has been focussed on the nano materials over bulk materials because of their novel physical and chemical properties [**1,2**]. Especially metal oxide nanoparticles have attracted interest because of their dramatic change in their physical and chemical properties [**1,2**]. Also, it has the application in various fields such as biosensors, catalysts, anticancer and antimicrobial agents [**1,2**]. Among these metal oxide nanoparticles, zinc oxide is widely employed because it's an essential microelement for humans which exists in proteins and enzymes [**3**]. It plays a significant role in biomedical applications such as drug delivery and bio imaging due to its non-toxic nature [**4**]. These biomedical properties are further enhanced by doping with transition elements such as copper, cobalt, nickel etc. Aluminum oxide nanoparticles have trapped the awareness of many researchers due to its great catalytic activities [**5**]. CuO nanoparticles has grabbed noteworthy attention because of its use as a potential fabrication of gas sensors [**6**]. The transition element co-doped ZnO can be used for treating diseases like hemophilia, genital blindness, viral infections, heart disease, diabetes and fungal infections [**7**]. Fungus infections can affect humans, animals and plant products. *Aspergillus* species causes disease in humans rarely but it leads to serious lung disease namely *Aspergillosis* [**8**].

It is also one of the most common causes of otomycosis (fungal ear infections) which can cause pain and temporary hearing loss [**9**]. *Aspergillus* species mainly affect plant products and food during the storage period and also these species frequently appear in tropical and subtropical regions than in temperate climates [**8**]. *Rizhopus* is a genus of common saprophytic fungi on plants and specialized parasites on animals. They are multicellular and found on a wide variety of organisms. Some *Rhizopus* species are opportunistic agents of human zygomycosis [**10**]. *Pencillium expansum* can cause severe post-harvest diseases in plants as grey and blue mold. It is also a major producer of *mycotoxin, patulin* which is commonly found in rotting apples [**11**].

Gold is chosen since it is an excellent antimicrobial agent [**12**]. Cobalt is chosen because iron and cobalt have the same physical and chemical properties and also, they are adjacent to each other in period 4 of the periodic table. ZnO nanoparticles Co-doped with Fe^{3+} and Pb^{2+} increases the antimicrobial activity against *E.coli* and *S.Aureus* bacteria [**13**]. The green synthesis of gold nanoparticles have fungicidal effect against *A.flavus* and *A.terreus* [**12**]. The Fe-ZnO shows the effective antifungal activity against *C.albicans* as compared to that of pure ZnO [**14**].

Fe doped ceria nanoparticles shows antifungal activity with MIC90 value of 0.48μg/mL against clinical isolates of *C.albicans* [**15**]. The Antifungal activity of C-doped ZnO nanostructures against *Rhizopus stolonifer* fungus has improved when compared to the undoped ZnO nanoparticles [**16**]. The pure and Fe doped ZnO nanoparticles exhibit antifungal activity against *Aspergillus*

niger, *Aspergillus flavus* and *Rhizopus* [**17**]. The effect and mode of action of iron-gold and cobalt-gold co-doped ZnO nanoparticles on the growth of such fungi have not yet been studied. Therefore, in this study, the antifungal activity of iron-gold and cobalt-gold co-doped ZnO against four important plant pathogenic fungi such as *Aspergillus niger*, *Aspergillus flavus*, *Rhizopus* and *pecillium* were investigated. Among various metal oxide nanoparticles, ZnO, iron - gold and cobalt - gold metals were chosen for present investigation because of its bio-compatibility and less toxicity [**18**].

Experimental

Materials

Zinc nitrate hexahydrate ($Zn(NO_3)_2.6H_2O$), polyethylene glycol (PEG400), Iron nitrate and Cobalt II chloride were purchased from HIMEDIA AR Grade, India. Gold (III) chloride was purchased from Sigma-Aldrich (99.9% pure). The detailed procedure adopted to synthesis the ZnO nanoparticle was described in the earlier study [**17**].

Synthesis of $Zn_{0.98}Fe_{0.01}Au_{0.01}O$ and $Zn_{0.98}Co_{0.01}Au_{0.01}O$ nanoparticles

The nanoparticles were synthesized through the sol-gel method without adding any reducing agents whereas PEG serves as a capping agent. For the preparation of $Zn_{0.98}Fe_{0.01}Au_{0.01}O$ nanoparticles, iron III nitrate and gold III chloride were used as the precursors of Fe^{3+} and $Au3^{+}$ salts respectively and $Zn(NO_3)_2.6H_2O$ as the source of zinc. 0.49 M of zinc nitrate hexahydrate, 0.005 M of iron III nitrate and gold III chloride were dissolved in 100 mL of distilled water. The hydrophobicity of PEG is responsible for the formation of mesoporous structure [**19**]. The solutions were mixed and stirred continuously for 2 hours using a magnetic stirrer. The pH value was adjusted to 7 by carefully adding polyethylene glycol. The solutions were heated at 60° C in continuous stirring for 3 hours. After stirring, the solution was kept at the same temperature for another 24 hours. The obtained powder was dried in the oven at 100° C for 24 hours and it was further calcined at 500° C in the furnace for 1 hour to obtain a nanocrystalline powder. The same procedure was followed to synthesize $Zn_{0.98}Co_{0.01}Au_{0.01}O$ NPs by using cobalt chloride as a precursor instead of iron nitrate.

Characterization of $Zn_{0.98}Fe_{0.01}Au_{0.01}O$ and $Zn_{0.98}Co_{0.01}Au_{0.01}O$ nanoparticles

The crystal structure and crystallite size of $Zn_{0.98}Fe_{0.01}Au_{0.01}O$ and $Zn_{0.98}Co_{0.01}Au_{0.01}O$ NPs were characterized by X-ray diffraction (XRD) study using Panalytical X'pert-Pro. The XRD instrument was functioned with monochromatic beam of Cu Kα radiation (1.5406 Å) in the 2θ range of 10˚-80˚. The transmittance spectrum of $Zn_{0.98}Fe_{0.01}Au_{0.01}O$ and $Zn_{0.98}Co_{0.01}Au_{0.01}O$ nanoparticles were recorded by UV-DRS spectra (Shimadzu UV-2450, USA) within 200-800 nm wavelength. The morphology of the NPs was examined by field emission – scanning electron microscope (FE-SEM; Carl Zeiss Microscopy, UK) and the elemental analysis was also performed along with FE-SEM analysis. The antifungal activity of the NPs was investigated against *Aspergillus niger*, *Aspergillus flavus*, *Rhizopus microsporus* and *Pencillium* sp using a well diffusion method on potato dextrose agar (PDA) medium. These fungi were grown in Actinomyces Isolation Media broth (Himedia Mumbai).

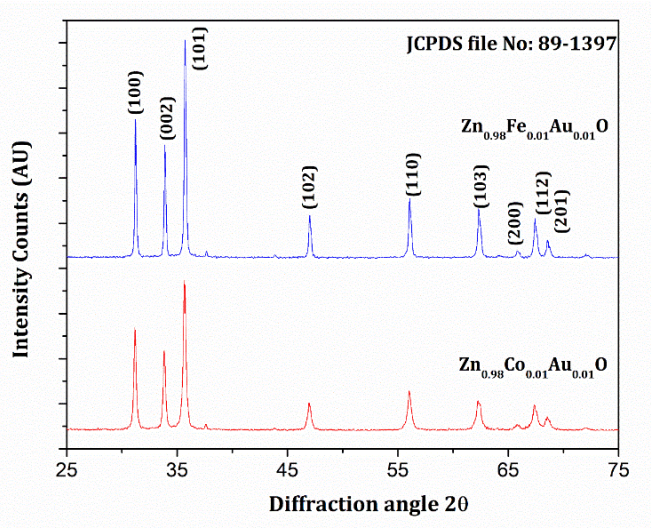

Fig. 1. XRD patterns of $Zn_{0.98}Fe_{0.01}Au_{0.01}O$ and $Zn_{0.98}Co_{0.01}Au_{0.01}O$ nanoparticles.

Results and discussion

The XRD patterns of $Zn_{0.98}Fe_{0.01}Au_{0.01}O$ and $Zn_{0.98}Co_{0.01}Au_{0.01}O$ NPs are shown in **Fig. 1**. The diffraction peaks occurred at 2θ = 36.1589, 31.6791 and 34.3842 and corresponded to hkl values (1 0 1), (1 0 0) and (0 0 2) confirm the existence of the wurzite crystal structure. There is a slight shift in the characteristic peaks of the doped $Zn_{0.98}Fe_{0.01}Au_{0.01}O$ and $Zn_{0.98}Co_{0.01}Au_{0.01}O$ nanoparticles. The average crystallite size of the nanoparticles were determined by the Scherrer's formula [**20**]. The crystallite size of $Zn_{0.98}Fe_{0.01}Au_{0.01}O$ and $Zn_{0.98}Co_{0.01}Au_{0.01}O$ NPs are 31.38 and 36.14 nm respectively.

UV–vis spectra of $Zn_{0.98}Fe_{0.01}Au_{0.01}O$ and $Zn_{0.98}Co_{0.01}Au_{0.01}O$ nanoparticles is shown in the **Fig. 2**. The absorption edge of $Zn_{0.98}Fe_{0.01}Au_{0.01}O$ and $Zn_{0.98}Co_{0.01}Au_{0.01}O$ nanoparticles are at 374 and 366 nm respectively. The corresponding band gap energies are 3.3151 and 3.3875 eV for $Zn_{0.98}Fe_{0.01}Au_{0.01}O$ and $Zn_{0.98}Co_{0.01}Au_{0.01}O$ nanoparticles respectively. The position of the absorption peak shifts towards the higher wavelength side when compared with the case of doped ZnO nanoparticles (362 nm and 3.425 eV). This indicates that the band gap of ZnO nanoparticles decreases by doping iron/gold and cobalt/gold nanoparticles. The decrease in band gap or red shift can be explained by the Burstein-Moss effect [**21**]. There will be a shift in the position of the absorption spectra towards the lower or higher wavelength

side while doping elements in ZnO. Generally, the doping of the transition metal with ZnO nanoparticles leads to decrease in band-gap of materials due to the sp-d interactions that exist due to the doping [**22-23**]. This phenomena can be explained on basis of the Burstein – Moss band filling effect [**23**] and this shift is due to the sp – d interactions between the band electrons of ZnO and the localized d electrons of the Fe ions [**23**]. Thus, the band gap decreases for the Fe doped ZnO samples than the Co doped ZnO one [**23**]. Therefore, it is expected that the band gap of $Zn_{0.98}Fe_{0.01}Au_{0.01}O$ and $Zn_{0.98}Co_{0.01}Au_{0.01}O$ nanoparticles decrease with a co-doping of iron-gold and cobalt-gold. The ZnO nanoparticle bandgap is reduced by adding doping iron / gold and cobalt / gold nanoparticles due to the addition of 3d transition elements such as Fe, Co to ZnO nanoparticles. This doping can alter Fermi's strength by raising the valance band and lowering the minimum conduction band leading to a reduction in the band gap. The narrowing of the band gap can be caused by the strong interaction of the s-d and p-d spin exchange interactions [**24**].

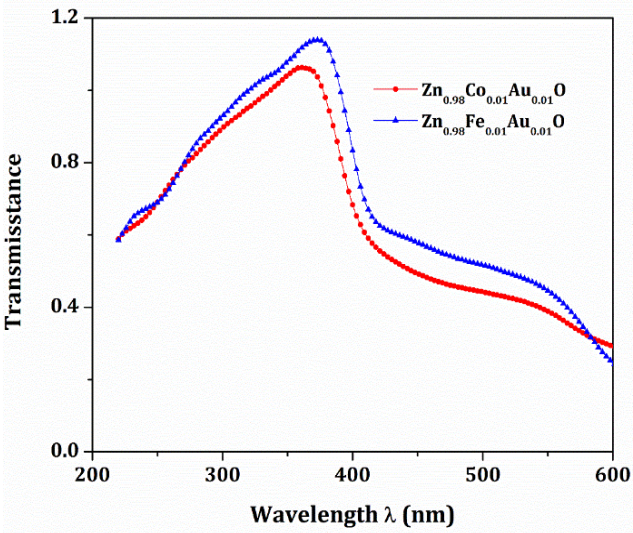

Fig. 2. UV – Vis spectra of $Zn_{0.98}Fe_{0.01}Au_{0.01}O$ and $Zn_{0.98}Co_{0.01}Au_{0.01}O$ nanoparticles.

The FE-SEM and EDX images of $Zn_{0.98}Fe_{0.01}Au_{0.01}O$ and $Zn_{0.98}Co_{0.01}Au_{0.01}O$ NPs have shown in **Fig. 3**. $Zn_{0.98}Co_{0.01}Au_{0.01}O$ and $Zn_{0.98}Fe_{0.01}Au_{0.01}O$ nanoparticles were smooth and spherical-like in shape. The EDX analysis were shown to confirm the presence of elemental zinc, oxygen, iron, cobalt and gold signals of $Zn_{0.98}Fe_{0.01}Au_{0.01}O$ and $Zn_{0.98}Co_{0.01}Au_{0.01}O$ nanoparticles. The atomic percentage of zinc, oxygen, iron and gold in $Zn_{0.98}Fe_{0.01}Au_{0.01}O$ nanoparticles were found to be 1, 0.981, 0.099 and 0.01 respectively. Similarly, the weight percentage of zinc, oxygen, cobalt and gold in $Zn_{0.98}Co_{0.01}Au_{0.01}O$ nanoparticles were found to be 1, 0.981, 0.01 and 0.01 respectively. Further, EDX analysis for $Zn_{0.98}Fe_{0.01}Au_{0.01}O$ and $Zn_{0.98}Co_{0.01}Au_{0.01}O$ nanoparticles shows that $Zn_{0.98}Co_{0.01}Au_{0.01}O$ has small variation in oxygen content [**25,26**].

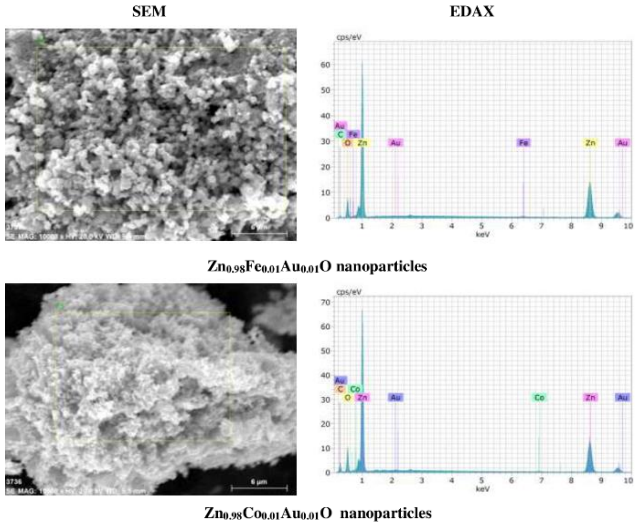

Fig. 3. SEM and EDAX spectra of $Zn_{0.98}Fe_{0.01}Au_{0.01}O$ and $Zn_{0.98}Co_{0.01}Au_{0.01}O$ nanoparticles.

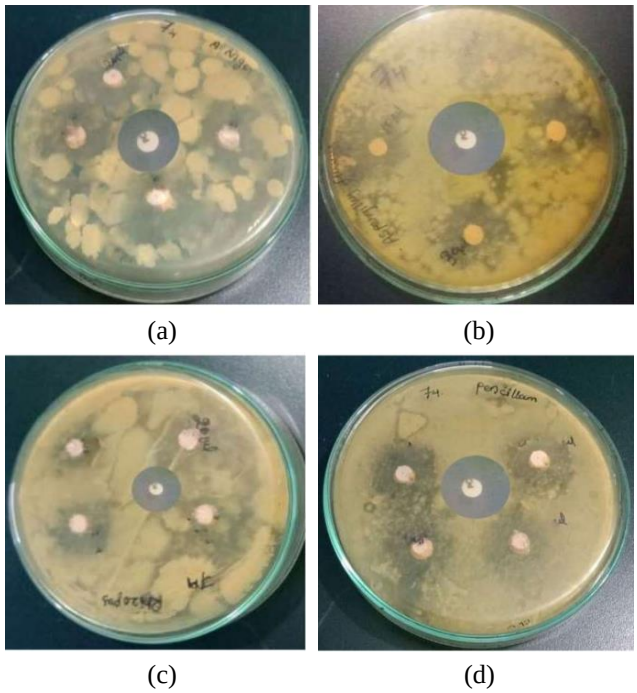

Fig. 4. Antifungal activity of $Zn_{0.98}Fe_{0.01}Au_{0.01}O$ nanoparticles at four different concentrations (10, 20, 30 and 40µl) against (a) *Aspergillus niger* (b) *Aspergillus flavus* (c) *Rhizopus* and (d) *Pencillium*

The antifungal activities of these nanoparticles were tested for the fungi such as *Aspergillus niger*, *Aspergillus flavus*, *Rhizopus microspores* and *Pencillium sp*. The antifungal activity of $Zn_{0.98}Fe_{0.01}Au_{0.01}O$ and $Zn_{0.98}Co_{0.01}Au_{0.01}O$ nanoparticles are shown in the **Fig. 4** and **Fig. 5**. It is clear from the figure that the $Zn_{0.98}Fe_{0.01}Au_{0.01}O$ and $Zn_{0.98}Co_{0.01}Au_{0.01}O$ nanoparticles acts an excellent antifungal agent against the fungi. **Table 1** depicts as the concentration of the nanoparticles increases from 10 µL to 40 µL the zone of inhibition values also increasing. The 40 µL concentration of $Zn_{0.98}Fe_{0.01}Au_{0.01}O$

nanoparticles has the zone of inhibition values 22 mm against *Aspergillus niger*, 20 mm against *Aspergillus flavus*, 22 mm against *Rhizopus* and 25 mm against *Pencillium*. Their standard zone of inhibition values are 18 mm, 19 mm, 18 mm and 18 mm respectively for *Aspergillus niger*, *Aspergillus flavus*, *Rhizopus* and *Pencillium*. Therefore, $Zn_{0.98}Fe_{0.01}Au_{0.01}O$ nanoparticles are more effective against all the above said fungi.

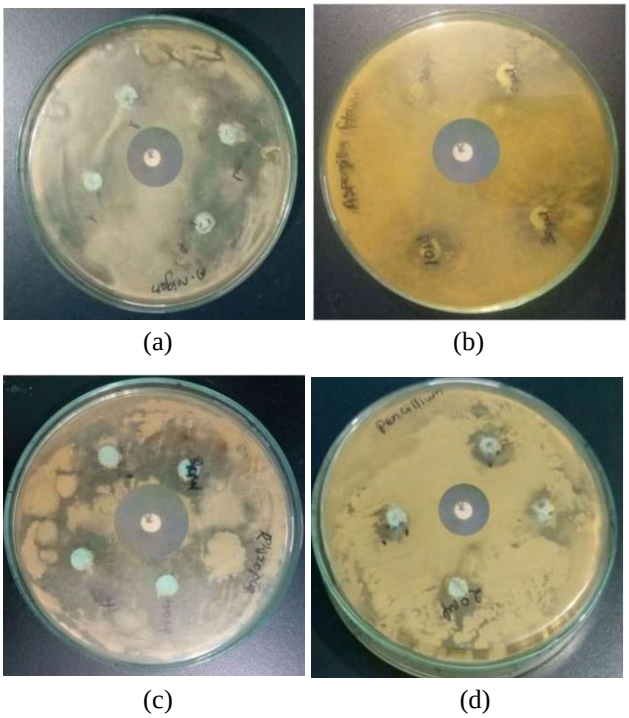

Fig. 5. Antifungal activity of $Zn_{0.98}Co_{0.01}Au_{0.01}O$ nanoparticles at four different concentrations (10, 20, 30 and 40µl) against (a) *Aspergillus niger* (b) *Aspergillus flavus* (c) *Rhizopus* and (d) *Pencillium.*

Among that these nanoparticles are most effective against *Pencillium* whose zone of inhibition is 25 mm. Similarly, 40 µL concentration of $Zn_{0.98}Co_{0.01}Au_{0.01}O$ nanoparticles has the zone of inhibition values 20 mm, 11 mm, 25 mm and 12 mm against *Aspergillus niger*, *Aspergillus flavus*, *Rhizopus* and *Pencillium* respectively. $Zn_{0.98}Co_{0.01}Au_{0.01}O$ nanoparticles are more effective against *Aspergillus niger* and *Rhizopus* fungi. In particular the $Zn_{0.98}Co_{0.01}Au_{0.01}O$ nanoparticles are more effective against *Rhizopus* and zone of inhibition value is found to be 25 mm.

Till now, there is no exact mechanism for the resistance to the fungus with nanoparticle. However, the various methodology and hypothesis were adopted to explain the interaction between nanoparticles and the membrane which causes pores on the membrane and the formation of the pores leads to the cell death. Especially, it was found from the literature that ZnO nanoparticles possess good antifungal activity against *Aspergillus nger* whose micro inhibition control value which is lower when compared with the fungus *B.Cineria* and *P.Expansum* [**27**]. While doping transition metal, there will be an enhancement in the antifungal activity [**17,21**]. In the case of pure and Fe doped ZnO nanoparticles shows better antifungal activity against *T.Mentagrophytes(s), C.Neoformans, A.Niger, A.Flavus* and *Rhizopus* [**17,21**]. When Au was doped in ZnO nanoparticles, the enhancement in the antimicrobial and antifungal activity was observed [**28**]. The increase is because of the nature of gold which facilitate the electron transfer between the Au doped ZnO nanorods and the micro-organisms [**28**]. A comparison showed that DNA cleavage of Au-ZnO nanorods was stronger than that of ZnO [**28**]. Au doped ZnO nanoparticles have antibacterial activity against *E.Coli, S.Aureus, E.Ashbyii, Bascillus Subtilis* as well as one fungal strain namely *Candida Albicans* [**28,29**].

Table 1. Comparative summaries of antifungal activity of $Zn_{0.98}Fe_{0.01}Au_{0.01}O$ and $Zn_{0.98}Co_{0.01}Au_{0.01}O$ nanoparticles.

Concentration (µL)	Zone of inhibition (mm)			
	A. niger	*A. flavus*	*R. microsporus*	*Pencillium* sp.
$Zn_{0.98}Fe_{0.01}Au_{0.01}O$ nanoparticles				
10	17	13	15	**18**
20	**18**	17	17	**20**
30	**20**	**19**	**19**	**22**
40	**22**	**20**	**22**	**25**
$Zn_{0.98}Co_{0.01}Au_{0.01}O$ nanoparticles				
10	12	7	**18**	5
20	16	9	**20**	8
30	**18**	10	**23**	10
40	**20**	11	**25**	12

A detailed mechanistic investigation of antifungal mechanism of nanoparticles synthesized by physical, chemical and biological methods are yet to be fully discovered [**21,30**]. The physical processes includes the interaction of nanoparticles directly with the microbial cell wall causing membrane dis-function and the interaction is due to the electrostatic attraction [**31,32**]. There will be desorption of ionic species from the nanoparticles and thereby generates reactive oxygen species (ROS) in the chemical phenomena through superoxide (O_2) anions, hydroxyl (OH) radicals and hydrogen per oxide (H_2O_2) which causes cell destruction [**31,32**]. The opposite charges of nanoparticles and fungus were indorsed to their bioactivity and adhesion due to electrostatic forces. In general, nanoparticle sizes has nearly monodispersed and mesoporous. Thus, because of the size of nanomaterials with fine surface roughness could use its whole surfaces through any direction to damage the cell membrane channels and blockage the transport property. An alternative mechanism, if there is positive ion released from the nanoparticles might attach to negatively charged fungus cell wall and rupture it, hence, leading to protein denaturation and cause death of cells [**33**]. The properties of ROS were due to the large surface area of nanoparticles

with its smaller particle size increases the oxygen vacancies [**32-34**].

In the biological processes, the incorporation of nanoparticles through ion channels or proteins at the cell wall results in the mechanical destruction of the cell membrane [**31,33**]. According to the experimental evidence and the literature, the most dominant mechanism responsible for the antifungal activity of ZnO nanoparticles are the chemical phenomena that is the generation of ROS [**31**]. The size of the microbes will be in micrometer range and their outer cell membrane will have pores of nanometer size [**31**]. The nanoparticles used in our work have size ranges from less than 50 nm. Therefore, it may penetrate in to the cell wall and damage the fungi from the interior [**31**]. Another possibility is the liberation of metal ions from the nanoparticles for example when ZnO is doped with fluorine the incorporation of F^- ions in the O^{2-} sites of the ZnO lattice increases the free electron concentration in ZnO which results in the increased generation of ROS thereby increases the antifungal activity [**31**]. Similarly, when nickel is doped in ZnO nanoparticles the incorporation of Ni^{2+} ions in Zn^{2+} ions increases the hole (h^+) concentration these h^+ reacts with H_2O and OH^- to produce $^{\cdot}OH$ radicals. The $^{\cdot}OH$ radicals is more oxidative than $^{\cdot}O_2^-$ radicals therefore there will be an enhancement in the antifungal activity [**29**]. In this study, the incorporation of Au and Co/Fe in Zn^{2+} ions increase the hole concentration thereby producing $^{\cdot}OH$ radicals and enhances the antifungal activity [**31-33**]. Thus, in this paper, the antibacterial activity of iron-gold and cobalt-gold doped with ZnO nanoparticles were successfully explored.

Conclusion

$Zn_{0.98}Fe_{0.01}Au_{0.01}O$ and $Zn_{0.98}Co_{0.01}Au_{0.01}O$ nanoparticles were synthesised and characterized. $Zn_{0.98}Fe_{0.01}Au_{0.01}O$ nanoparticles exhibit high antifungal activity against *Aspergillus niger*, *Aspergillus flavus*, *Rhizopus microsporus* and *Pencillium sp*. The reported antifungal activity is higher than that of the standard antibiotic *Nystatin*. Whereas $Zn_{0.98}Co_{0.01}Au_{0.01}O$ nanoparticles are highly active against *Aspergillus niger* and *Rhizopus* whose antifungal activity is also higher than that of *Nystatin*. Therefore, these nanoparticles can be used to treat the fungal infections in humans, animals and plants.

Keywords

Gold nanoparticles, Structural properties, Optical properties, Antifungal activity, Aspergillus niger, Aspergillus flavus, Rhizopus, Pencillium sp.

Received: 9 September 2020
Revised: 14 November 2020
Accepted: 27 November 2020

References

1. Ahmad, I.; Mazhar, M.E.; Usmani, M.N.; Khan, K.; Ahmad, S.; Ahmad, J.; *Mater Res Express*, **2018**, *6*, 35014.
2. Pugazhendhi, A.; Prabhu, R.; Muruganantham, K.; Shanmuganathan, R.; Natarajan, S.; *J. Photochem Photobiol B Biol*. **2019**, *190*, 86.
3. Miri, A.; Mahdinejad, N.; Ebrahimy, O.; Khatami, M.; Sarani, M.; *Mater Sci Eng C*., **2019**, *104*, 109981.
4. Khalil, A.T.; Ovais, M.; Ullah, I.; et. al. *Nanomedicine*, **2017**, *12*, 1767.
5. Jay A. Tanna; Chaudhary, Ratiram Gomaji; et. al, *Adv. Mater. Lett.*, **2016**, *7*, 933. Tanna, J. A.; Chaudhary, R. G.; Gandhare, N. V.; Juneja, H. D.; *Adv. Mater. Lett.*, **2016**, *7*, 100.
6. Potbhare, Ajay K.; Chaudhary, Ratiram Gomaji; Chouke, Prashant B.; Yerpude, Sachin; Mondal, Aniruddha; Sonkusare, Vaishali N.; Rai, Alok R.; Juneja. Harjeet D.; *Materials Science and Engineering: C*, **2019**, *99*, 783.
7. Naveed Ul Haq A.; Nadhman, A.; Ullah, I.; Mustafa, G.; Yasinzai, M.; Khan, I.; *J. Nanomater*., **2017**, *2017*, 8510342.
8. Samson, R.A.; Houbraken, J.; Summerbell, R.C.; Flannigan, B.; Miller, J.D.; Common and important species of fungi and actinomycetes in indoor environments. Microorg home indoor Work Environ Divers Heal impacts, Investig Control. Published online **2002**, 285-473.
9. de W Blackburn C.; Food Spoilage Microorganisms. Woodhead Publishing; **2006**.
10. Ownley, B.H.; Gwinn, K.D.; Vega, F.E.; *BioControl*., **2010**, *55*, 113.
11. He, L.; Liu, Y.; Mustapha, A.; Lin, M.; *Microbiol Res*., **2011**, *166*, 207.
12. Eskandari-Nojedehi, M.; Jafarizadeh-Malmiri, H.; Rahbar-Shahrouzi, J.; *Green Process Synth*., **2018**, *7*, 38.
13. Andrade Neto, N.F.; Matsui, K.N.; Paskocimas, C.A.; Bomio, MRD; Motta, F.V.; *Mater Sci Semicond Process*., **2019**, *93*, 123.
14. Chai, H.Y.; Lam, S.M.; Sin, J.C.; *Mater Lett*., **2019**, *242*, 103.
15. Rahdar, A.; Aliahmad, M.; Samani, M.; Heidari Majd, M.; Susan, MABH; *Ceram Int*., **2019**, *45*, 7950.
16. Decelis, S.; Sardella, D.; Triganza, T.; Brincat, J.P.; Gatt, R.; Valdramidis, V.P.; *Royal Society Open Science*, **2017**, *4*, 161032.
17. Ferin Fathima, A.; Jothi Mani, R.; Sakthipandi, K.; Manimala, K.; Hossain, A.; *J. Inorg Organomet Polym Mater*., **2020**, *30*, 2397.
18. Iriarte-Mesa, Claudia, Yeisy C. López, Yasser Matos-Peralta, Karen de la Vega-Hernández, and Manuel Antuch; "Gold, Silver and Iron Oxide Nanoparticles: Synthesis and Bionanoconjugation Strategies Aimed at Electrochemical Applications." Topics in Current Chemistry, **2020**, *378(1)*, pp.1-40.
19. Sonkusare, Vaishali N.; Chaudhary, Ratiram Gomaji; Bhusari, Ganesh S.; Mondal, Aniruddha; Potbhare, Ajay K.; Mishra, Raghvendra Kumar; Juneja, Harjeet D.; Abdala, Ahmed A.; *ACS Omega*, **2020**, *5*, 7823.
20. Sakthipandi, K.; Rajendran, V.; *Mater Charact*., **2013**, *77*, 70.
21. Sharma, N.; Jandaik, S.; Kumar, S.; Chitkara, M.; Sandhu, I.S.; *J. Exp. Nanosci*., **2016**, *11*, 54.
22. Nair, M.G.; Nirmala, M.; Rekha, K.; Anukaliani, A.; *Mater Lett*. **2011**, *65*, 1797.
23. Kumar, S.; Mukherjee, S.; Kr. Singh R.; Chatterjee, S.; Ghosh, A.K.; *J. Appl Phys*., **2011**, *110*, 103508.
24. Srinivasulu, T.; Saritha, K.; Ramakrishna Reddy, K. T.; *Modern Electronic Materials*, **2017**, *3*, 76.
25. Abdul Salam, H.; Sivaraj, R.; Venckatesh, R.; *Mater Lett*., **2014**, *131*, 16.
26. Jayaseelan, C.; Rahuman, A.A.; Kirthi, A.V.; et. al. *Spectrochim Acta Part A Mol Biomol Spectrosc*, **2012**, *90*, 78.
27. Jamdagni, P.; Khatri, P.; Rana, J.S.; *J. King Saud Univ - Sci*., **2018**, *30*, 168.
28. Bazrafshan, A.A.; Ghaedi, M.; Hajati, S.; Naghiha, R.; Asfaram, A.; *Ecotoxicol Environ Saf*., **2017**, *142*, 330.
29. Pathak, T.K.; Kroon, R.E.; Swart, H.C.; *Vacuum*, **2018**, *157*, 508.
30. Kumari, M.; Giri, V.P.; Pandey, S.; et. al. *Pestic Biochem Physiol*., **2019**, *157*, 45.
31. Kumar, R.S.; Dananjaya, SHS.; De Zoysa M.; Yang M.; *RSC Adv*., **2016**, *6*, 108468.
32. Bagade, Reena; Chaudhary, Ratiram Gomaji; Potbhare, Ajay; Mondal, Aniruddha; Desimone, Martin; Dadure, Kanhaiya; Mishra, Raghvendra; Juneja, Harjeet; *ChemistrySelect*, **2019**, *4*, 6233.
33. Sondi, Ivan; Branka Salopek-Sondi; *Journal of Colloid and Interface Science*, **2004**, *275*, 177.
34. Sonkusare, Vaishali N.; Chaudhary, Ratiram Gomaji; Bhusari, Ganesh S.; Mondal, Aniruddha; Potbhare, Ajay K.; Mishra, Raghvendra Kumar; Juneja, Harjeet D.; Abdala, Ahmed A.; *ACS Omega*, **2020**, *5*, 7823.